Clinical Pharmacokinetics (2025) 64:1495–1506
https://doi.org/10.1007/s40262-025-01544-x

ORIGINAL RESEARCH ARTICLE

Pharmacokinetics, Pharmacodynamics, and Urinary Recovery of Oral Mescaline Hydrochloride in Healthy Participants

Lorenz Mueller[1,2] · Aaron Klaiber[1,2] · Laura Ley[1,2] · Anna M. Becker[1,2] · Jan Thomann[1,2] · Dino Luethi[1,2] · Yasmin Schmid[1,2] · Matthias E. Liechti[1,2]

Accepted: 22 June 2025 / Published online: 14 July 2025

Abstract

Background and Objective Mescaline is a classic serotonergic psychedelic with a long history of human use. The present study analyzed the pharmacokinetics, pharmacokinetic-pharmacodynamic relationship, and urinary recovery of oral mescaline hydrochloride.

Methods Data from 105 single-dose administrations (100–800 mg) in 49 participants from two phase I trials were analyzed with compartmental pharmacokinetics and pharmacokinetic-pharmacodynamic modeling. A one-compartment model with first-order absorption, elimination, and a lag time was used to describe mescaline plasma concentrations. Acute subjective effects, assessed by visual analog scales (range 0–100%), were modeled using a sigmoid E_{max} model linked to plasma concentrations via a first-order rate constant (k_{e0}).

Results Mescaline showed dose-proportional increases in total exposure and maximal concentrations, with a peak concentration reached within 2.0 h (geometric mean) and a half-life of 3.5 h across all doses. Mean model-predicted onset of "any drug effect" occurred around 1 hour post-dose. Maximum predicted effect intensity and duration increased with dose, from 13% and 2.8 h at 100 mg to 89% and 15 h at 800 mg. Over all conditions, 53% of the dose was excreted into urine unchanged, and 31% was excreted as the main metabolite 3,4,5-trimethoxyphenylacetic acid over 24–30 h.

Conclusions These findings provide the first detailed pharmacokinetic-pharmacodynamic characterization of mescaline in humans and indicate an oral bioavailability of at least 53%, limited by first-pass metabolism to 3,4,5-trimethoxyphenylacetic acid, followed by predominant renal elimination of both analytes.

Clinical Trial Registration ClinicalTrials.gov identifier: NCT04227756 and NCT04849013.

1 Introduction

Mescaline (3,4,5-trimethoxyphenethylamine) is a psychedelic phenethylamine alkaloid that is naturally found in different species of cacti, such as the North American peyote (*Lophophora williamsii*) and South American San Pedro (*Echinopsis pachanoi*) [1]. It is considered a classic serotonergic psychedelic like lysergic acid diethylamide (LSD), psilocybin, and *N,N*-dimethyltryptamine, defined by a shared common mechanism of action as agonists at the serotonin 5-hydroxytryptamine-2A (5-HT_{2A}) receptor [2, 3]. The 5-HT_{2A} receptor antagonist ketanserin blocked acute psychedelic effects of mescaline in humans [4].

Interest in psychedelics has surged in recent years, prompting studies to explore their clinical pharmacology in healthy participants [5–8] and evaluate their therapeutic potential for various psychiatric conditions [9–15]. Most of these trials have focused on psilocybin and LSD, but very few have investigated mescaline [16].

Among classic psychedelics, mescaline has the lowest affinity for 5-HT_{2A} receptors [3, 17–19]. The low affinity of mescaline for 5-HT_{2A} receptors [3] and poor blood–brain barrier permeability [20] contribute to the comparatively high oral doses of 300–800 mg of mescaline hydrochloride (HCl) that are typically required to induce a full psychedelic

Lorenz Mueller and Aaron Klaiber have contributed equally to the study.

✉ Matthias E. Liechti
matthias.liechti@usb.ch

[1] Division of Clinical Pharmacology and Toxicology, Department of Biomedicine and Department of Clinical Research, University Hospital Basel and University of Basel, Schanzenstrasse 55, CH-4056 Basel, Switzerland

[2] Department of Pharmaceutical Sciences, University of Basel, Basel, Switzerland

Key Points

The study describes the pharmacokinetic-pharmacodynamic relationship and urinary recovery of oral mescaline hydrochloride single doses in healthy participants using a non-compartmental analysis and compartmental modeling.

A one-compartment model with first-order absorption and elimination, as well as a lag time described mescaline plasma concentrations well. Mescaline showed dose linearity between 100 and 800 mg. Subjective effects were linked to plasma concentrations using a first-order rate constant (k_{e0}) to account for a pharmacokinetic-pharmacodynamic delay.

After an oral first-pass metabolism to its main metabolite 3,4,5-trimethoxyphenylacetic acid, renal excretion seems to be the primary eliminatory route of both mescaline and 3,4,5-trimethoxyphenylacetic acid. The oral mescaline bioavailability could be indirectly estimated and is at least 53%. The present data can be used in future studies with mescaline to define dosing in healthy participants and patients, especially with impaired renal function.

experience in humans compared with psilocybin dihydrate (20–40 mg) and LSD base (100–200 µg) [5, 21].

Only limited data on the pharmacology of mescaline in humans have been available until now. The only earlier study used ^{14}C-labeled mescaline HCl to study the metabolism of mescaline in 12 healthy male subjects using an oral dose of 500 mg of mescaline HCl [22]. Our group recently investigated the acute effects, pharmacology, and safety of different oral mescaline HCl doses in healthy participants across two separate trials [4, 21, 23], providing the first modern controlled data on mescaline in humans. In the present study, we report urinary recovery data from these trials for the first time, improving our understanding of the metabolism and elimination of mescaline. Pharmacokinetic-pharmacodynamic (PK-PD) modeling was previously used by our group to describe PK-PD relationships of LSD and psilocybin [6, 7, 24–26]. The present study was also the first to investigate the pharmacokinetics and PK-PD relationship of mescaline in humans using compartmental modeling.

2 Methods

2.1 Study Design

The present analysis included data from two different previously published studies that were conducted in healthy volunteers at the University Hospital Basel [4, 21]. Overall, we analyzed data from 113 mescaline HCl administrations in 49 individuals.

In Study 1, 32 participants were included. Sixteen participants received 300 mg of mescaline HCl, and 16 participants received 500 mg of mescaline HCl. Study 1 compared the acute subjective effects of oral single doses of LSD (100 µg), psilocybin (20 mg), mescaline HCl (300 or 500 mg), and placebo in a randomized double-blind crossover design [21]. Because of weaker acute subjective effects at 300 mg of mescaline compared with LSD (100 µg) and psilocybin (20 mg) in the first 16 participants, the mescaline HCl dose was increased to 500 mg for the second 16 participants. Only data of the mescaline conditions were used for the present analysis.

Study 2 investigated acute subjective effects of different oral doses of mescaline HCl in 17 participants using a randomized double-blind crossover design [4]. Each participant received single doses of mescaline HCl (100, 200, 400, and 800 mg) and a combination of mescaline HCl (800 mg) with ketanserin (40 mg). One participant dropped out after experiencing distress during the first session (800 mg of mescaline HCl) and was excluded from within-subject comparisons [4] but was retained in the present analysis. The co-administration of mescaline HCl (800 mg) with ketanserin (40 mg) markedly reduced the acute subjective response to mescaline and mescaline-induced emesis compared with 800 mg of mescaline HCl alone. Frequent emesis after administration of the highest dose of mescaline HCl (800 mg) may have reduced the absorption of mescaline [4]. In the present analysis, we included the mescaline and ketanserin condition in the PK analysis but not in the PK-PD analysis.

The washout periods between sessions were at least 10 or 14 days for Studies 1 and 2, respectively [4, 21]. All participants provided written informed consent and received compensation for their participation. Both studies were approved by the local ethics committee and registered at ClinicalTrials.gov (NCT04227756 and NCT04849013). The research was conducted in accordance with the Declaration of Helsinki and International Conference on Harmonization Guidelines for Good Clinical Practice. Approval for administering psychedelics to healthy participants was granted by the Swiss Federal Office for Public Health, Bern, Switzerland.

2.2 Participants

Physically and mentally healthy people, 25–65 years of age with a body mass index of 18–29 kg/m^2, were eligible for the studies. Key exclusion criteria were pregnancy, breastfeeding, a personal or first-degree relative history of major psychiatric disorders, chronic somatic illness, and/or the use of medications that might interfere with the studies. Complete

inclusion and exclusion criteria are provided in the Electronic Supplementary Material (ESM).

2.3 Study Drug

Mescaline HCl was synthesized by ReseaChem GmbH, Burgdorf, Switzerland. In both studies, capsules that contained 100 mg of mescaline HCl and identical capsules that contained mannitol as placebo were produced according to Good Manufacturing Practice (Apotheke Dr. Hysek, Biel, Switzerland). The exact analytical contents of mescaline HCl in the dosing units, together with the corresponding calculated mescaline contents that were used as dosing inputs for all analyses, are provided in the ESM.

2.4 Study Procedures

After providing written informed consent, the eligibility of participants was assessed at a screening visit based on a medical history, physical examination, psychiatric assessment, electrocardiogram, vital parameters, and analyses of blood chemistry and hematology. The included participants attended four 25-h or six 31-h dosing sessions in Studies 1 and 2, respectively. Dosing sessions were conducted in a calm hospital room and began at 8 a.m. with baseline measurements and a standardized small breakfast. The study medication was administered at 9 a.m., after which outcome measures were repeatedly assessed for 24 or 30 h, respectively. The participants remained under constant supervision during the acute effect phase, and an investigator spent the night in the room next to the participants. After all sessions, an end-of-study visit was conducted to assess the overall study experience and the participants' health status [4, 21].

2.5 Blood and Urine Samples

Blood samples were drawn and collected into lithium heparin tubes 0, 0.25, 0.5, 0.75, 1, 1.5, 2, 3, 3.5, 4, 5, 6, 7, 8, 10, 12, 14, 16, and 24 h after dosing for Study 1 and 0, 0.5, 1, 1.5, 2, 3, 4, 5, 6, 8, 9, 10, 11, 12, 14, 16, 20, 24, and 30 h after dosing for Study 2. Blood samples were immediately centrifuged, and plasma was stored at −80 °C until analysis. In Study 1, urine was collected over time intervals of 8 h (0–8, 8–16, and 16–24 hours). In Study 2, urine was collected cumulatively from 0 to 30 h after dosing. Urine samples were frozen and stored at −80 °C until analysis. Cases of incomplete urinary sampling because of strong psychedelic effects were excluded from the analysis. Concentrations of mescaline and its metabolites 3,4,5-trimethoxyphenylacetic acid (TMPAA) and *N*-acetylmescaline (NAM) were determined by a fully validated, high-performance liquid chromatography-tandem mass spectrometry method [27].

2.6 Acute Subjective Effects

Single-item visual analog scales (VASs), presented as 100-mm horizontal lines (0–100%) and marked from "not at all" on the left to "extremely" on the right, were repeatedly used to assess acute subjective effects over time. The VASs included "any drug effect," "good drug effect," "bad drug effect," "nausea," and "the boundaries between me and my surroundings seem to blur," the latter measuring "ego dissolution" (i.e., loss of sense of self), a subjective effect that is characteristic of psychedelics [5, 8, 28–30]. In both studies, VASs were administered at the same timepoints as blood samples were drawn [4, 21].

2.7 PK Analyses and PK-PD Modeling

All analyses were performed using Phoenix WinNonlin 8.4 (Certara, Princeton, NJ, USA) using the actual sampling times. Doses were adjusted to the analytically exact content of mescaline in the capsules. For urinary recovery, molar doses and concentrations were used. As vomiting could lead to incomplete absorption after oral drug administration, profiles were excluded if emesis occurred within 1 hour after dosing or up to 1 h after the observed peak plasma (C_{max}) concentration.

We first conducted non-compartmental analyses (NCAs) for mescaline, TMPAA, and NAM. Peak plasma concentration and time to C_{max} (t_{max}) were obtained directly from the observed data. The terminal elimination rate constant (λ_z) to calculate the half-life ($t_{1/2}$) was estimated by log-linear regression after semilogarithmic transformation of the data using at least three data points of the linear phase of the concentration–time curve. The area under the concentration–time curve from 0 to the last post-dosing timepoint was computed by employing the linear-up log-down method. The infinite area under the concentration–time curve (AUC_∞) was derived by extrapolating the area under the concentration–time curve from 0 to the last post-dosing timepoint using the constant λ_z. Because the two studies used different sampling timepoints, we report the AUC_∞ together with the percentage of extrapolation of the AUC_∞. Total (μmoL) and relative (% of dose) urinary recovery was calculated for mescaline and its metabolites. Renal clearance (L/h) was calculated as urinary recovery/AUC_∞.

Subsequently, we conducted sequential compartmental PK and PK-PD modeling of mescaline plasma concentrations and acute effects. Datasets were modeled individually for each participant and condition. All models were developed using the naïve pooled engine in Phoenix WinNonlin, which applies a quasi-Newton Broyden–Fletcher–Goldfarb–Shanno algorithm to minimize the −2 Log likelihood (−2LL) objective function. A stepwise approach was applied to evaluate model performance using visual fits of

predicted versus measured concentrations/effects, the −2LL, Akaike information criteria (AIC), coefficients of variation of parameter estimates, parameter correlations, and residual error plots during the model fitting process. The addition of a parameter to the model was evaluated using likelihood ratio tests by comparing the difference −2LL values between nested models. Statistical significance was determined using the chi-squared distribution with degrees of freedom equal to the number of additional parameters in the more complex model. A drop of 3.84 in the −2LL value was considered statistically significant for the addition of one parameter, corresponding to a p-value of 0.05. We counted the number of profiles showing a significant improvement. Further, the mean, standard deviation (SD), and 95% confidence intervals (CIs) of the differences in −2LL and AIC across individual profiles were calculated. Plasma concentrations below the lower limit of quantification occurring before dose administration were manually set to zero. Post-dose below the lower limit of quantification values were handled using a censored likelihood approach equivalent to the M3 method [31], implemented in Phoenix WinNonlin.

For the PK model development, a one-compartment model with first-order absorption and first-order elimination was initially created after visual inspection of raw plasma concentrations of mescaline. The addition of a lag time (t_{lag}) to account for dissolution of the capsule after oral administration, and of a second compartment was evaluated as described above. The absorption rate constant (k_a), t_{lag}, apparent clearance (Cl/F), and apparent volume of distribution (V_d/F) were the primary estimated model parameters. Secondary parameters were derived as follows: $k_e = (Cl/F)/(V_d/F)$, $t_{max} = \log\ (k_a/k_e)/(k_a–k_e) + t_{lag}$, $C_{max} = Dose/V_d\ e^{-(ke(tmax-tlag))}$, $AUC = dose/(V_d/F)/k_e$, $t_{1/2} = \ln 2/k_e$. A multiplicative residual error model was used to account for proportional residual variability.

After fitting the PK model, a combined PK-PD model was developed. Individually estimated PK parameters were frozen for PK-PD modeling. For the PD modeling, the VAS item "any drug effect" was used as the primary outcome. A sigmoid maximum effect (E_{max}) model (EC_{50}, E_{max}) with an E_{max} of 100%, according to the range of VASs from 0 to 100% was selected. The addition of a steepness parameter (γ) and a first-order equilibrium rate constant (k_{e0}), connecting plasma concentration to a virtual effect compartment, was evaluated using the same stepwise process described above. An additive residual error model was used for the PD effects. The PK-PD model was developed primarily for the VAS item "any drug effect," which reflects the overall effect strength. The same model structure was then applied to the VAS items "good drug effect" and "ego dissolution." These measures include further emotional components of the experience that depend on a variety of other factors partly independent of the mescaline plasma concentration and are to be considered explorative. "Bad drug effect" and "nausea" showed a poor correlation with plasma concentrations and were not modeled. EC_{50}, k_{e0}, and γ were determined as primary model PD parameters. The secondary PD parameters area under the effect-time curve, maximal reached effects (E_{max}), time of E_{max} (t_{maxE}), time of effect onset (t_{onset}), and effect duration were derived using an NCA on the model-predicted individual effect-time profiles at 10-min intervals. This NCA applied linear trapezoidal integration for calculation of the area under the effect-time curve and a threshold of 10% of the individual E_{max} for estimation of t_{onset} and effect duration. Primary and secondary model parameters were then summarized using standard statistics.

3 Results

3.1 Participants

Characteristics of the participants who were included in the present study are shown in Table S1 of the ESM. Overall, 49 participants (25 female, 24 male) with a mean ± SD age of 30 ± 7 years were included in the present analysis. A total of 34 participants (69%) had prior experience with psychedelics (five ± four times).

Early vomiting occurred in eight participants (1 after 400 mg, 5 after 800 mg, and 2 after 800 mg plus ketanserin). After exclusion of these profiles, data from a total of 105 administrations remained in the final analysis.

3.2 Results from the NCA and Urinary Recovery

Urinary recovery data are provided in Table 1. Over all conditions, 53% (geometric mean) of the administered dose was recovered as unchanged mescaline and 31% as TMPAA. In Study 1, the total and relative recovery of mescaline and TMPAA was nominally lower than in Study 2, where almost the complete dose was recovered. More than 50% of recovered mescaline, TMPAA, and NAM appeared in urine in the first 8 h after dose administration, with diminishing amounts at later time intervals (Table S4 of the ESM).

Both mescaline and TMPAA showed dose linearity between 100 and 800 mg (Fig. S1 and Table S2 of the ESM). Mescaline and TMPAA exhibited very similar concentration–time profiles, characterized by rapid absorption and comparable C_{max}, t_{max}, and $t_{1/2}$. This is further illustrated by individually plotting raw concentrations of both analytes (Fig. S3 of the ESM). Peak plasma concentration and AUC values of NAM were considerably lower and <10% compared with mescaline.

3.3 Model Building

A one-compartment model with first-order absorption and elimination was initially built to describe mescaline pharmacokinetics. The addition of a second compartment did not improve the visual fit, and while a significant drop in −2LL was observed in 40 out of 105 profiles, the two volumes of distribution were strongly correlated. We therefore discarded the second compartment. Adding a lag time parameter improved the visual fit around C_{max} in many profiles and led to a significant improvement in −2LL in 59 out of 105 profiles. Mean ± SD (95% CI) differences across profiles were 11 ± 12 (8.4–13) for −2LL and 8.7 ± 12 (6.4–11) for AIC, supporting the inclusion of the lag parameter in the final PK model.

For the PK-PD model, a simple E_{max} model was initially evaluated, but it substantially underestimated peak effects and overestimated later responses. Adding a sigmoidicity parameter (y) greatly improved the visual fit and resulted in a significant drop in −2LL in 81 out of 91 profiles. A k_{e0} parameter was subsequently tested to account for a counterclockwise hysteresis observed in the concentration-effect data (Fig. S2 of the ESM). This addition further improved the visual fit, particularly at peak effect times, and led to a significant drop in −2LL in 74 out of 91 profiles. Mean ± SD (95% CI) differences across profiles were 30 ± 25 (20–35) for −2LL and 28 ± 25 (23–33) for AIC, favoring the inclusion of k_{e0} in the final PK-PD model.

3.4 Results from PK and PK-PD modeling

Figure 1a presents the geometric mean of model-predicted mescaline concentrations over time, and Table 2 summarizes the corresponding primary and secondary PK parameters. The interindividual variability of drug exposure is illustrated in overlayed individual predictions over time in Fig. S5 of the ESM. The PK model successfully captured concentration–time profiles of mescaline, and the results aligned well with the NCA (Table S2 of the ESM). Model diagnostic plots and curves of individual estimated versus observed concentrations that illustrate the visual fit are provided in Figs. S4 and S6 of the ESM, respectively.

Mean model-predicted subjective effect-time curves for single-item VAS ratings of "any drug effect," "good drug effect," and "ego dissolution" are illustrated in Fig. 1b–d. Figure 2 shows the interindividual variability of "any drug effect" by plotting individual predicted effect-time curves. Corresponding plots for "good drug effect" and "ego dissolution" are provided in Figs. S10 and S13 of the ESM. Diagnostic plots for all PK-PD models and individual curves of observed versus predicted effects over time are provided in Figs. S7–9, S11–12, and S14 of the ESM. Primary and secondary parameters of the PK-PD

Table 1 Urinary recovery and renal clearance of mescaline and TMPAA

		Dose (μmol)	*n*	Mescaline			TMPAA			Total
				Cl/F (L/h)	Total recovery (μmol)	% of dose recovered	Renal Cl (L/h)	Total recovery (μmoL)	% of dose recovered	Renal Cl (L/h)	% of dose recovered
Study	**Condition**										
2	M-100	390	16	45 (42–47)	204 (181–229)	52 (46–58)	23 (20–26)	181 (166–196)	46 (42–49)	24 (20–28)	99 (90–108)
2	M-200	780	15	45 (42–47)	439 (405–474)	56 (51–60)	25 (22–28)	314 (291–338)	40 (37–42)	21 (18–23)	96 (89–102)
1	M-300	1143	15	36 (33–38)	524 (487–563)	45 (41–48)	16 (14–17)	238 (213–265)	20 (17–22)	8.8 (8.0–9.7)	66 (61–70)
2	M-400	1559	15	43 (39–46)	924 (849–1004)	59 (54–64)	25 (22–27)	589 (511–678)	37 (32–42)	20 (17–22)	97 (88–106)
1	M-500	1913	16	44 (39–49)	887 (763–1030)	47 (40–55)	21 (18–24)	391 (333–458)	20 (16–23)	10 (8.3–12)	68 (57–79)
2	M-800	3113	11	41 (38–43)	1617 (1356–1928)	52 (43–61)	21 (16–26)	928 (740–1162)	29 (23–36)	15 (11–19)	82 (68–98)
2	M-800-K	3122	14	40 (36–43)	1985 (1818–2166)	63 (57–68)	25 (21–28)	1081 (981–1190)	34 (30–37)	18 (15–20)	98 (90–105)
All conditions			102	42 (40–43)	708 (612–818)	53 (50–55)	22 (20–23)	418 (368–474)	31 (28–33)	16 (14–17)	85 (80–89)

Data are presented as geometric mean with 95% confidence intervals in brackets, 800-K refers to the 800 mg of mescaline + 40 mg of ketanserin condition

Cl/F apparent total clearance from the NCA, *h* hour, *n* number of profiles with both blood and urine data, *NCA* non-compartmental analysis, *TMPAA* 3,4,5-trimethoxyphenylacetic acid, *renal Cl* renal clearance calculated by dividing urinary recovery/infinite area under the concentration–time curve (data from the NCA)

model are presented in Table 3. In profiles where observed effects were consistently very low or remained at zero, the estimated EC_{50} values were extreme outliers, often unreasonably high. To avoid skewing, profiles with estimated maximal effects <1% were excluded from the summary statistics for primary PD parameters. However, for the calculation of secondary PD parameters using an NCA of predicted effect-time profiles, these profiles were retained. Their low predicted effects over time were deemed valid as they predicted the zero effects and excluding them might have led to an overestimation of the effects. Again, a good alignment between acute drug effects that were predicted by the PK-PD model and those from the NCA (Table S3 of the ESM) was observed. Mean model-predicted "any drug effects" started around 1 hour after dosing, and maximal effects were reached between 1.9 (100 mg) and 4.2 h (500 mg). Maximal effect strength and effect duration for "any drug effect" increased with higher doses from 13% and 2.8 h (100 mg) to 89% and 15 h (800 mg), respectively.

4 Discussion

The present study was the first to analyze the pharmacokinetics and PK-PD relationship of orally administered mescaline HCl in humans and the first to report modern human data of mescaline urinary recovery, covering a broad dosing range between 100 and 800 mg. We analyzed 105 complete and richly sampled PK profiles using compartmental modeling of combined data from two previously published studies in 49 healthy volunteers.

Mescaline exhibited dose-proportional increases in AUC and C_{max} from 100 to 800 mg. A one-compartment model that used first-order absorption and elimination, as well as a lag time to account for dissolution of the gelatine capsule, adequately predicted plasma mescaline concentrations over time for all doses. Mescaline showed rapid oral absorption, with maximal plasma concentrations that were reached 2.0 h (geometric mean) after administration and a lag time of 0.2 h. Estimated half-lives in plasma were around 3.5 h for all doses. Overall, model-predicted parameters were in good alignment with results from the NCA.

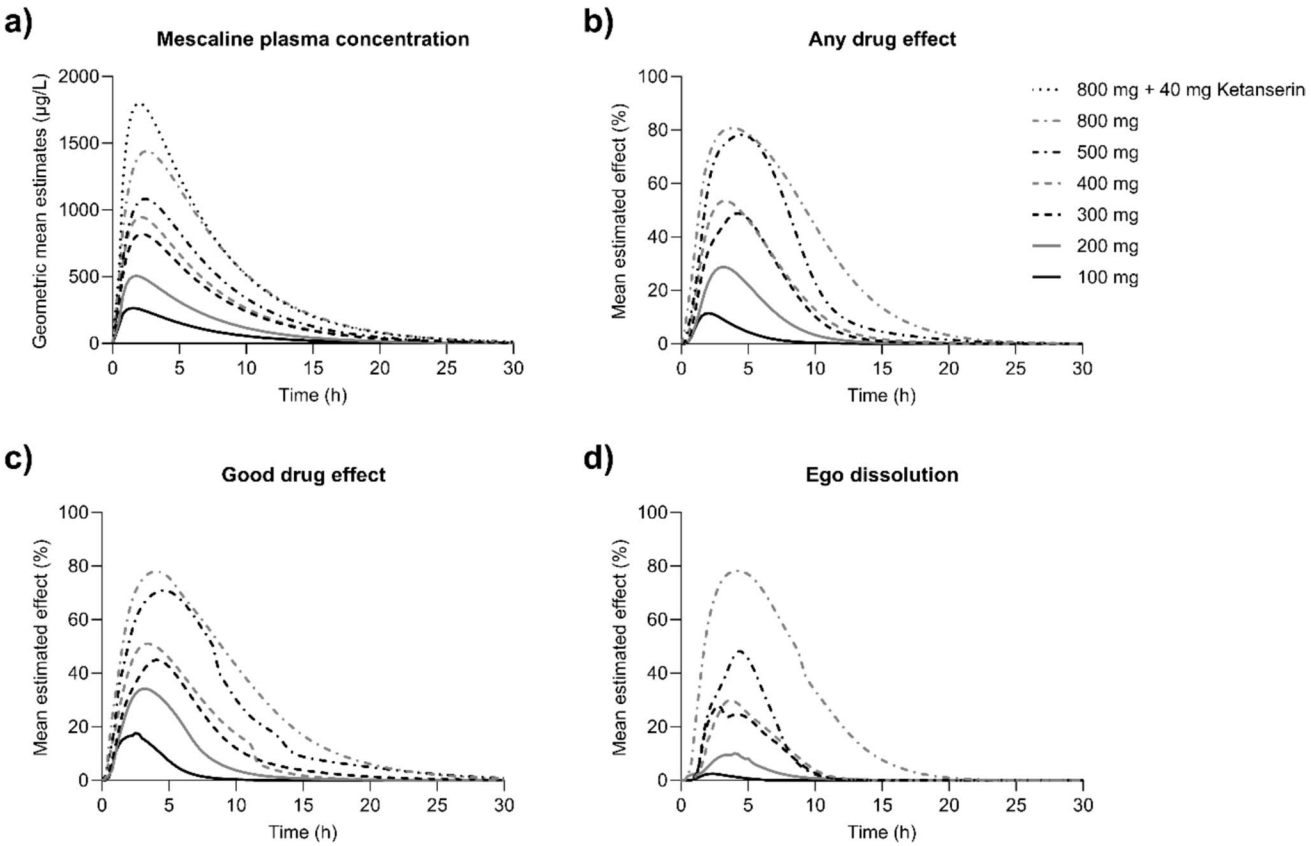

Fig. 1 Results of the pharmacokinetic (**a**) and pharmacokinetic-pharmacodynamic (**b–d**) models for different doses of mescaline. **a** Model-predicted plasma concentrations of mescaline over time (geometric mean over a total of 105 individual profiles). **b–d** Model-predicted acute subjective effects over time (mean over a total of 91 individual profiles) for **b** "any drug effect," **c** "good drug effect," and **d** "ego dissolution." *h* hours

Table 2 Pharmacokinetic parameters of mescaline determined by compartmental modeling

Study	Dose (mg)	*n*	Primary model parameters				Secondary model parameters			
			k_a (1/h)	t_{lag} (h)	Cl/F (L/h)	V_d/F (L)	C_{max} (µg/L)	t_{max} (h)	AUC (h*µg/L)	$t_{1/2}$ (h)
2	100	16	2.59 (1.54–4.35)	0.19 (0.10–0.29)	46 (43–49)	225 (207–245)	284 (258–312)	1.3 (0.93–1.7)	1803 (1699–1912)	3.4 (3.2–3.7)
2	200	16	1.67 (1.26–2.23)	0.25 (0.16–0.34)	46 (43–50)	233 (216–252)	521 (487–558)	1.7 (1.5–2.0)	3553 (3308–3817)	3.5 (3.2–3.8)
1	300	16	0.96 (0.76–1.21)	0.15 (0.09–0.21)	37 (34–40)	191 (173–211)	826 (748–913)	2.2 (2.0–2.5)	6533 (6045–7061)	3.6 (3.3–3.9)
2	400	15	1.10 (0.83–1.47)	0.17 (0.07–0.26)	43 (40–48)	223 (207–240)	1001 (927–1080)	2.1 (1.7–2.5)	7575 (6906–8308)	3.6 (3.3–3.8)
1	500	16	0.80 (0.59–1.08)	0.18 (0.12–0.24)	45 (40–50)	214 (180–255)	1124 (1034–1223)	2.4 (2.1–2.8)	9037 (8114–10065)	3.3 (2.9–3.8)
2	800	12	0.74 (0.47–1.16)	0.19 (0.11–0.28)	42 (38–45)	220 (185–262)	1778 (1599–1977)	2.6 (2.1–3.2)	15765 (14471–17174)	3.7 (3.1–4.3)
2	800-K	14	1.49 (0.92–2.43)	0.27 (0.17–0.37)	41 (37–45)	218 (199–239)	2164 (1911–2451)	1.9 (1.5–2.4)	16038 (14558–17668)	3.7 (3.5–3.9)
All doses										
		105	1.24 (1.07–1.44)	0.20 (0.17–0.23)	43 (41–44)	217 (209–226)		2.0 (1.8–2.1)		3.5 (3.4–3.6)

K_a, t_{lag}, Cl/F, and V_z/F are primary parameters determined by the model; C_{max}, t_{max}, AUC, and $t_{1/2}$ are secondary model parameters derived from the primary parameters as described in the methods section

Data are presented as geometric mean with 95% confidence intervals in brackets, 800-K refers to the 800 mg of mescaline + 40 mg of ketanserin condition. The analytically exact mescaline content per dose is listed in the ESM

AUC area under the concentration–time curve, *Cl/F* apparent total clearance, C_{max} maximum estimated plasma concentration, *h* hours, k_a absorption rate constant, *n* number of profiles, $t_{1/2}$ plasma half-life, t_{lag} lag time, t_{max} time of C_{max}, V_z/F apparent volume of distribution

Mescaline and its main metabolite TMPAA showed very similar concentration–time profiles. The early and similar t_{max} and C_{max} for both analytes could best be attributed to a first-pass metabolism of approximately 50% of the oral dose. After this first-pass metabolism, only limited further mescaline metabolism appeared to occur, illustrated by a parallel decline of concentrations of mescaline and TMPAA and the fact that 53% of the total administered dose was recovered as unchanged mescaline in urine over all doses. Additionally, our urinary recovery data showed, that in many cases, nearly 100% of the administered dose was excreted as either mescaline or TMPAA over 24–30 h. Assuming an oral bioavailability of about 50% for mescaline, the observed renal clearance of 22 L/h would essentially represent the total clearance. This aligns with the Cl/F of 42 L/h being reduced to approximately 21 L/h when corrected for bioavailability (i.e., 42 L/h × 0.5). Despite their similar concentration–time profiles, the recovery of TMPAA was lower than mescaline, particularly in Study 1. This study used a sampling time of 24 h, whereas sampling in Study 2 continued up to 30 h. However, most of the recovered TMPAA in Study 1 appeared in urine early, with only 5.2–9.2% of the total amount recovered between 16 and 24 h for 300 and 500 mg, respectively. We assume only small amounts were excreted beyond 24 h. In Study 1 (300 mg), we also observed higher dose-corrected area under the concentration–time curve values, which — together with the lower recovery — resulted in lower renal clearance estimates for mescaline and TMPAA. The cause of these inconsistencies is unclear, but they may be partly explained by differences in the participant populations between the two studies.

Several further metabolites in addition to TMPAA have previously been described [32]. *N*-acetylmescaline is one such metabolite, which could also be quantified in the present study, but concentrations were very low, and the elimination half-life of ~2 h was comparatively short. Based on these findings, NAM is unlikely to be of clinical relevance. No further minor metabolites were determined in the present study.

Based on our data, we conclude that the oral bioavailability of mescaline is at least 53%, with first-pass metabolism to TMPAA likely accounting for the reduction. Following first-pass metabolism, mescaline is primarily excreted unchanged in urine. This likely has implications in cases where renal function is impaired. Furthermore, the calculated renal clearance of mescaline was 22 L/h or 366 mL/min over all doses, which is higher than typical glomerular filtration rates in healthy adults, possibly indicating active secretion. In contrast to mescaline, LSD is entirely (99%) metabolized, inactivated, and eliminated, likely independent of renal function [7].

Only limited data on the pharmacology of mescaline in humans have been available until now. The only earlier study

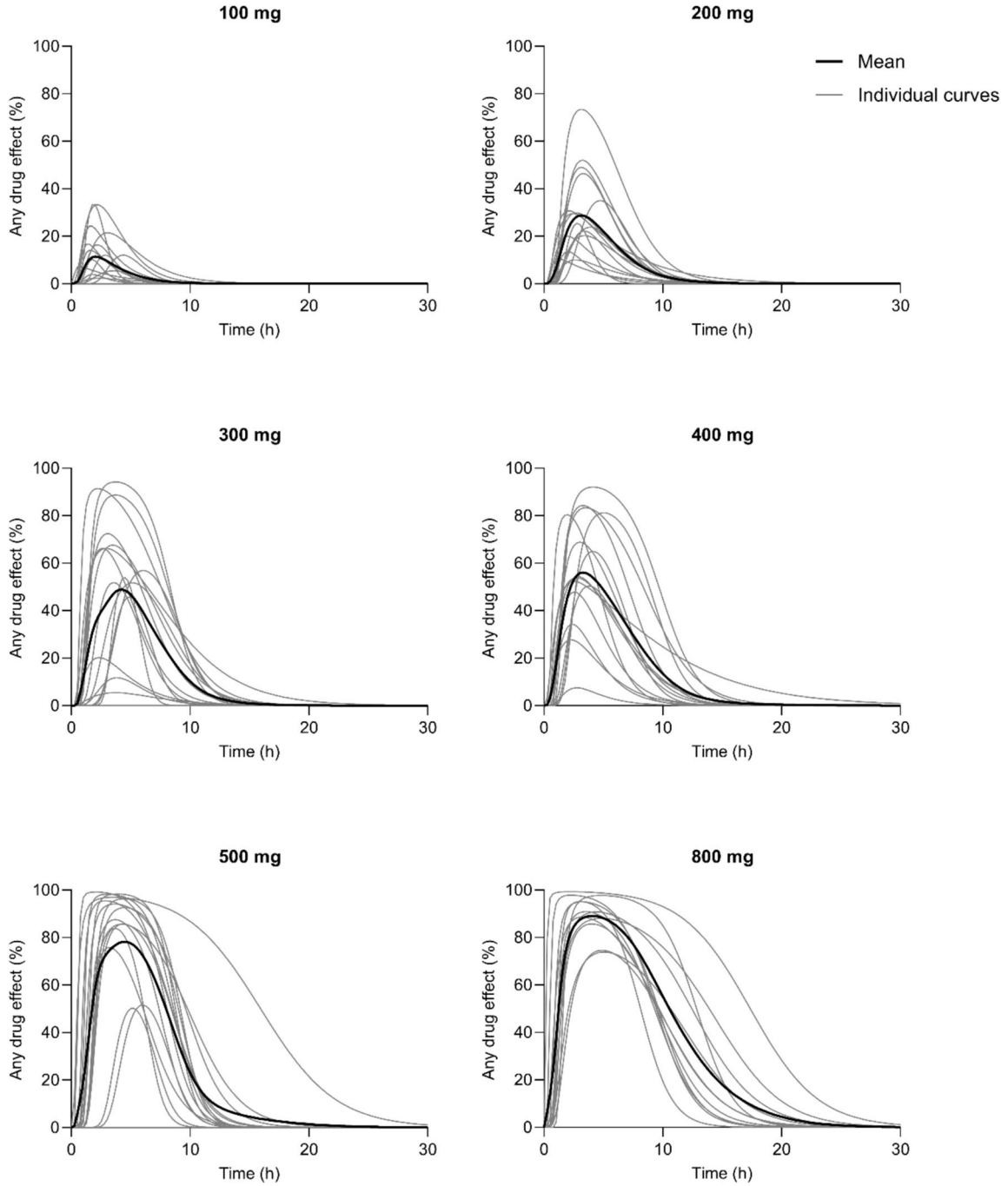

Fig. 2 Mean (*bold black line*) and individual (*gray lines*) model-predicted curves of "any drug effect" over time for different doses of mescaline. *h* hours

used ^{14}C-labeled mescaline HCl to study the metabolism of mescaline in 12 healthy male subjects using an oral dose of 500 mg of mescaline HCl [22]. The biological half-life of the ingested radioactivity was approximately 6 hours, whereas we consistently observed shorter half-lives of both mescaline (3.5–3.8 h) and TMPAA (3.7–4.1 h). In this previous study, 87% of the ingested radioactivity was excreted in urine within 24 h, and 92% was excreted within 48 h [22], similar to our observed rates of total recovery. Mescaline was mainly excreted unchanged in urine (55–60%), and the main metabolite was TMPAA (27–30%), which was confirmed by our findings.

We found that acute subjective effects of mescaline were closely linked to the plasma mescaline concentrations but

Table 3 Pharmacodynamic parameters of mescaline derived by compartmental pharmacokinetic-pharmacodynamic modeling

Study	Dose (mg)	Primary model parameters				Secondary parameters derived by the NCA of predicted effects					Effect duration (h)
		n	EC_{50} (µg/L)	γ	k_{e0} (1/h)	*n*	AUEC (h*%)	E_{max} (%)	t_{onset} (h)	t_{maxE} (h)	
VAS "any drug effect"											
2	100	13	506 (361–652)	3.8 (2.8–4.9)	2.5 (1.4–3.7)	16	44 (25–64)	13 (8.1–18)	0.8 (0.5–1.1)	1.9 (1.4–2.5)	2.8 (1.6–3.9)
2	200	14	687 (531–843)	2.8 (2.1–3.5)	1.6 (0.9–2.3)	16	157 (107–208)	30 (22–39)	0.9 (0.7–1.1)	2.9 (2.5–3.3)	7.1 (6.0–8.2)
1	300	14	712 (487–937)	3.8 (2.7–4.9)	1.7 (0.7–2.7)	16	321 (209–433)	52 (38–67)	1.3 (0.9–1.7)	3.5 (2.8–4.2)	8.0 (6.1–9.8)
2	400	14	844 (665–1023)	2.9 (2.3–3.5)	1.8 (0.9–2.6)	15	383 (280–487)	58 (46–70)	0.8 (0.6–1.0)	3.1 (2.7–3.5)	9.8 (8.1–11)
1	500	15	602 (500–704)	4.9 (3.9–6.0)	1.3 (0.9–1.7)	16	608 (440–776)	80 (67–93)	1.4 (0.9–1.9)	4.2 (3.5–5.0)	10 (7.8–12)
2	800	12	680 (543–817)	3.0 (2.1–4.0)	1.6 (0.9–2.3)	12	948 (785–1112)	89 (85–94)	0.7 (0.5–0.9)	3.8 (3.2–4.4)	15 (13–17)
All doses		82	673 (605–741)	3.5 (3.1–3.9)	1.7 (1.4–2.0)	91			1.1 (1.0–1.2)	3.2 (2.9–3.5)	
VAS "good drug effect"											
2	100	12	495 (252–737)	4.3 (3.1–5.5)	3.3 (1.2–5.4)	16	68 (19–118)	18 (5.7–31)	0.9 (0.5–1.3)	1.8 (1.1–2.5)	2.6 (1.3–3.9)
2	200	15	737 (480–995)	3.3 (2.2–4.3)	1.2 (0.8–1.5)	16	194 (125–263)	35 (23–47)	0.9 (0.7–1.1)	2.8 (2.4–3.3)	7.4 (5.9–9.0)
1	300	14	794 (463–1126)	4.8 (3.1–6.5)	1.8 (0.4–3.2)	16	333 (170–497)	48 (33–64)	1.5 (0.9–2.0)	4.1 (2.8–5.4)	8.0 (5.0–11)
2	400	15	933 (701–1164)	2.8 (2.1–3.6)	2.1 (1.0–3.2)	15	395 (262–529)	56 (44–68)	0.8 (0.5–1.1)	3.0 (2.4–3.6)	9.9 (8.4–11)
1	500	14	570 (436–703)	4.7 (2.9–6.6)	1.4 (0.6–2.2)	16	665 (419–910)	72 (57–87)	1.2 (0.8–1.6)	3.6 (2.9–4.3)	11 (7.6–14)
2	800	12	733 (558–908)	2.6 (1.5–3.7)	2.4 (1.1–3.8)	12	925 (733–1117)	81 (76–87)	0.8 (0.6–1.0)	4.1 (3.6–4.7)	15 (13–20)
All doses		82	718 (618–818)	3.7 (3.2–4.3)	2.0 (1.5–2.5)	91			1.1 (0.9–1.2)	3.2 (2.9–3.6)	
VAS "ego dissolution"											
2	100	4	359 (161–558)	9.0 (1.9–16)	2.1 (0.6–3.6)	16	7.6 (– 1.2–16)	2.8 (– 0.2–5.9)	1.7 (0.3–3.0)	0.7 (0.03–1.4)	0.5 (– 0.1–1.1)
2	200	10	525 (434–616)	7.0 (3.8–10)	1.4 (– 0.1–2.9)	16	49 (12–86)	13 (5.6–20)	2.2 (1.5–2.9)	2.2 (1.2–3.2)	2.5 (0.8–4.3)
1	300	12	742 (634–849)	11 (4.7–18)	2.1 (0.8–3.4)	16	153 (52–254)	38 (20–56)	1.8 (1.2–2.4)	2.6 (1.7–3.5)	3.4 (1.6–5.1)
2	400	11	921 (746–1096)	7.1 (2.9–11)	1.4 (0.7–2.1)	15	171 (72–270)	38 (22–53)	1.7 (1.4–1.9)	3.3 (2.6–4.0)	4.4 (2.6–6.2)
1	500	12	876 (753–1000)	11 (8.4–15)	1.1 (0.5–1.8)	16	230 (125–336)	53 (33–72)	2.2 (1.6–2.7)	3.4 (2.5–4.3)	4.1 (2.6–5.6)
2	800	12	834 (702–966)	4.3 (2.6–6.1)	1.4 (1.0–1.9)	12	800 (674–926)	90 (85–94)	1.0 (0.8–1.2)	4.1 (3.4–4.8)	12 (10–14)
All doses		61	758 (690–826)	8.3 (6.5–10)	1.5 (1.1–1.9)	91			1.7 (1.5–2.0)	2.6 (2.2–3.0)	

For primary model parameters, profiles with E_{max}<1% were excluded (see also the results section). For the secondary NCA of effects over time, all profiles were used. A threshold of 10% of individual E_{max} was used to determine t_{onset} and effect duration. Data are presented as means with 95% confidence intervals in brackets. The analytically exact mescaline content per dose is listed in the ESM

AUEC area under the effect-time curve, EC_{50} effect-site concentration that produces half-maximal effects, E_{max} maximal estimated effects, k_{e0} first-order effect-site to blood equilibrium rate constant, *h* hours, *n* number of included profiles, *NCA* non-compartmental analysis, t_{maxE} time of E_{max}, t_{onset} time to reach threshold effects, *VAS* visual analog scale, γ sigmoid shape parameter

occurred with a delay as seen in the counterclockwise hysteresis. Accordingly, our modeling approach that used an effect compartment that was connected to the plasma mescaline concentration using a first-order equilibrium rate constant (k_{e0}) adequately described the observed acute effects. This finding is consistent with a delayed central distribution of mescaline. Notably, similar results could have been obtained for TMPAA, given the close relationship between its plasma concentrations and those of mescaline. However, the TMPAA metabolite has previously been shown to be inactive [33].

Similar modeling approaches were previously used to describe PK-PD relationships of LSD and psilocybin [6, 7, 24–26]. The PK-PD relationship of mescaline is similar to LSD and psilocybin and consistent with the view that these 5-HT_{2A} receptor agonists produce subjective effects provided they are present in the plasma/brain and occupy the 5-HT_{2A} receptor [7, 25, 34–36].

The present study has several strengths. A large and complete set of richly sampled data over a wide dose range was analyzed. Our studies used highly controlled settings and analytically confirmed doses of mescaline HCl. The combination of PK and urinary recovery data allowed an indirect first estimation of oral mescaline bioavailability.

However, several limitations should be noted. Our healthy and mostly young sample limits external validity, especially in older people or patients with impairments in kidney function. Prior experience with psychedelics may have some influence on the participants' PD response. Methodological differences between the two studies may have influenced the total recovery of mescaline and its metabolites. Study 1 analyzed two different cohorts of 16 participants for the 300- and 500-mg doses, whereas Study 2 used a crossover design where the participants received all doses. The estimated PK lag time was low, and its addition did not significantly improve the model fit in 46/105 profiles. This may be because of rapid absorption with t_{max} being the first or second measured concentration, as the studies were not primarily designed to model the absorption phase. The significance of the lag parameter could further be evaluated using a population-based PK-PD modeling approach. Additionally, in PD profiles with minimal or no observed effects, estimated EC_{50} values were estimated unrealistically high and therefore excluded from the summary statistics. A population-based approach could have addressed this issue more effectively and allowed for a further differentiation between intra- and interindividual variability. We used a sigmoid E_{max} model to describe the PD effects assessed by VASs. While this approach has a mechanistic background given that the acute subjective effects of mescaline are primarily mediated through 5-HT_{2A} receptor agonism, which follows a sigmoidal binding relationship, it remains a simplification. Most importantly, it ignores downstream biochemical, neurophysiological, and emotional processes that contribute to the subjective experience and its intensity. To confirm our estimation of the oral bioavailability of mescaline, an additional intravenous administration of mescaline would be needed in a future study.

5 Conclusions

Mescaline exhibited dose-proportional pharmacokinetics and was well described by a one-compartment model with first-order absorption and elimination. The subjective effects were closely related to the course of plasma concentrations within subjects with a short response lag and according to a sigmoidal E_{max} model and without evidence of acute tolerance. The data are consistent with an oral bioavailability of mescaline HCl of at least 53% due to first-pass metabolism to TMPAA, and renal excretion appears to be the primary route of elimination of both mescaline and TMPAA.

Supplementary Information The online version contains supplementary material available at https://doi.org/10.1007/s40262-025-01544-x.

Acknowledgements The authors thank F. Holze, D. Arikci, I. Straumann, L. Erne, A. Jelušić, S. Dierbach, and F. Coviello for their help with conducting the clinical studies and M. Arends for proofreading the manuscript.

Declarations

Funding Open access funding provided by University of Basel. This work was supported by the Swiss National Science Foundation (grant no. 32003B_185111 to MEL), University Hospital Basel, and Mind Medicine, Inc. The expertise and data associated with this work and owned by the University Hospital Basel were licensed by Mind Medicine, Inc. Mind Medicine, Inc., had no role in planning or conducting the present study or writing the present publication.

Conflicts of Interest/Competing Interests Matthias E. Liechti is a consultant for Mind Medicine, Inc. Lorenz Mueller, Aaron Klaiber, Laura Ley, Anna M. Becker, Jan Thomann, Dino Luethi, and Yasmin Schmid have no conflicts of interest that are directly relevant to the content of this article.

Ethics Approval Both included trials were approved by the local ethics committee (Ethikkokmmission Nordwest- und Zentralschweiz, EKNZ) and registered at ClinicalTrials.gov (NCT04227756 and NCT04849013).

Consent to Participate All participants provided written informed consent.

Consent for Publication All participants provided written informed consent.

Availability of Data and Materials The datasets presented in this article are not readily available because the data associated with this work are owned by the University Hospital Basel and were licensed by Mind

Medicine Inc. Requests to access the datasets should be directed to Matthias E. Liechti, matthias.liechti@usb.ch.

Code Availability Not applicable.

Authors' Contributions YS and MEL designed the studies. LM analyzed the data. LM and AK wrote the manuscript. AK, LL, and AB performed the research. JT and DL validated the analytical method and analyzed the PK samples. All authors revised and gave final approval for the manuscript.

References

1. Dinis-Oliveira RJ, Pereira CL, da Silva DD. Pharmacokinetic and pharmacodynamic aspects of Peyote and mescaline: clinical and forensic repercussions. Curr Mol Pharmacol. 2019;123:184–94.
2. Nichols DE. Psychedelics. Pharmacol Rev. 2016;682:264–355.
3. Rickli A, Moning OD, Hoener MC, et al. Receptor interaction profiles of novel psychoactive tryptamines compared with classic hallucinogens. Eur Neuropsychopharmacol. 2016;26:1327–37.
4. Klaiber A, Schmid Y, Becker AM, et al. Acute dose-dependent effects of mescaline in a double-blind placebo-controlled study in healthy subjects. Transl Psychiatry. 2024;14:395.
5. Holze F, Ley L, Müller F, et al. Direct comparison of the acute effects of lysergic acid diethylamide and psilocybin in a double-blind placebo-controlled study in healthy subjects. Neuropsychopharmacology. 2022;476:1180–7.
6. Holze F, Becker AM, Kolaczynska KE, et al. Pharmacokinetics and pharmacodynamics of oral psilocybin administration in healthy participants. Clin Pharmacol Ther. 2023;1134:822–31.
7. Holze F, Erne L, Duthaler U, et al. Pharmacokinetics, pharmacodynamics and urinary recovery of oral lysergic acid diethylamide administration in healthy participants. Br J Clin Pharmacol. 2024;90:200–8.
8. Holze F, Vizeli P, Ley L, et al. Acute dose-dependent effects of lysergic acid diethylamide in a double-blind placebo-controlled study in healthy subjects. Neuropsychopharmacology. 2021;463:537–44.
9. Holze F, Gasser P, Muller F, et al. Lysergic acid diethylamide-assisted therapy in patients with anxiety with and without a life-threatening illness: a randomized, double-blind, placebo-controlled phase II study. Biol Psychiatry. 2023;933:215–23.
10. von Rotz R, Schindowski EM, Jungwirth J, et al. Single-dose psilocybin-assisted therapy in major depressive disorder: a placebo-controlled, double-blind, randomised clinical trial. EClinicalMedicine. 2023;56:101809.
11. Carhart-Harris R, Giribaldi B, Watts R, et al. Trial of psilocybin versus escitalopram for depression. N Engl J Med. 2021;38415:1402–11.
12. Griffiths RR, Johnson MW, Carducci MA, et al. Psilocybin produces substantial and sustained decreases in depression and anxiety in patients with life-threatening cancer: a randomized double-blind trial. J Psychopharmacol. 2016;3012:1181–97.
13. Davis AK, Barrett FS, May DG, et al. Effects of psilocybin-assisted therapy on major depressive disorder: a randomized clinical trial. JAMA Psychiat. 2021;785:481–9.
14. Goodwin GM, Aaronson ST, Alvarez O, et al. Single-dose psilocybin for a treatment-resistant episode of major depression. N Engl J Med. 2022;38718:1637–48.
15. Bogenschutz MP, Ross S, Bhatt S, et al. Percentage of heavy drinking days following psilocybin-assisted psychotherapy vs placebo in the treatment of adult patients with alcohol use disorder: a randomized clinical trial. JAMA Psychiat. 2022;7910:953–62.
16. Vamvakopoulou IA, Narine KAD, Campbell I, et al. Mescaline: the forgotten psychedelic. Neuropharmacology. 2023;222:109294.
17. Kovacic P, Somanathan R. Novel, unifying mechanism for mescaline in the central nervous system: electrochemistry, catechol redox metabolite, receptor, cell signaling and structure activity relationships. Oxid Med Cell Longev. 2009;24:181–90.
18. Cassels BK, Saez-Briones P. Dark classics in chemical neuroscience: mescaline. ACS Chem Neurosci. 2018;910:2448–58.
19. Ray TS. Psychedelics and the human receptorome. PLoS ONE. 2010;52: e9019.
20. Páleníček T, Balíková M, Bubeníková-Valešová V, et al. Mescaline effects on rat behavior and its time profile in serum and brain tissue after a single subcutaneous dose. Psychopharmacology. 2008;1961:51–62.
21. Ley L, Holze F, Arikci D, et al. Comparative acute effects of mescaline, lysergic acid diethylamide, and psilocybin in a randomized, double-blind, placebo-controlled cross-over study in healthy participants. Neuropsychopharmacology. 2023;4811:1659–67.
22. Charalampous W, Walker KE, Kinross-Wright J. Metabolic fate of mescaline in man. Psychopharmacologia. 1966;9:48–63.
23. Klaiber A, Humbert-Droz M, Ley L, et al. Safety pharmacology of acute mescaline administration in healthy participants. Br J Clin Pharmacol. 2024. https://doi.org/10.1111/bcp.16349.
24. Dolder PC, Schmid Y, Steuer AE, et al. Pharmacokinetics and pharmacodynamics of lysergic acid diethylamide in healthy subjects. Clin Pharmacokinet. 2017;56:1219–30.
25. Holze F, Duthaler U, Vizeli P, et al. Pharmacokinetics and subjective effects of a novel oral LSD formulation in healthy subjects. Br J Clin Pharmacol. 2019;85:1474–83.
26. Holze F, Liechti ME, Hutten N, et al. Pharmacokinetics and pharmacodynamics of lysergic acid diethylamide microdoses in healthy participants. Clin Pharmacol Ther. 2021;1093:658–66.
27. Thomann J, Ley L, Klaiber A, et al. Development and validation of an LC-MS/MS method for the quantification of mescaline and major metabolites in human plasma. J Pharm Biomed Anal. 2022;220:114980.
28. Holze F, Vizeli P, Müller F, et al. Distinct acute effects of LSD, MDMA, and D-amphetamine in healthy subjects. Neuropsychopharmacology. 2020;453:462–71.
29. Roseman L, Nutt DJ, Carhart-Harris RL. Quality of acute psychedelic experience predicts therapeutic efficacy of psilocybin for treatment-resistant depression. Front Pharmacol. 2017;8:974.
30. Preller KH, Vollenweider FX. Phenomenology, structure, and dynamic of psychedelic states. Curr Top Behav Neurosci. 2016;36:221–56.
31. Beall JR. A teratogenic study of chlorpromazine, orphenadrine, perphenazine, and LSD-25 in rats. Toxicol Appl Pharmacol. 1972;212:230–6.
32. Dinis-Oliveira RJ. Metabolism of psilocybin and psilocin: clinical and forensic toxicological relevance. Drug Metab Rev. 2017;491:84–91.

33. Charalampous KD, Orengo A, Walker KE, et al. Metabolic fate of beta-(3,4,5-trimethoxyphenyl)-ethalamine (mescaline) in humans: isolation and identification of 3,4,5-trimehoxyphenylacetic acid. J Pharmacol Exp Ther. 1964;145:242–6.
34. Holze F, Madsen MK, Svarer C, et al. Ketanserin exhibits dose- and concentration-proportional serotonin 2A receptor occupancy in healthy individuals: relevance for psychedelic research. Eur Neuropsychopharmacol. 2024;88:43–8.
35. Madsen MK, Fisher PM, Burmester D, et al. Psychedelic effects of psilocybin correlate with serotonin 2A receptor occupancy and plasma psilocin levels. Neuropsychopharmacology. 2019;447:1328–34.
36. Becker AM, Klaiber A, Holze F, et al. Ketanserin reverses the acute response to LSD in a randomized, double-blind, placebo-controlled, crossover study in healthy participants. Int J Neuropsychopharmacol. 2023;262:97–106.